International Journal of Modern Physics and Applications
Vol. 7, No. 1, 2021, pp. 6-11
http://www.aiscience.org/journal/ijmpa
ISSN: 2381-6945 (Print); ISSN: 2381-6953 (Online)

Magnetohydrodynamic Prandtl-Eyring Fluid Flow Along Porous Plates with Slip Effects

Oyelami Funmilayo Helen*

Department of Mathematical and Physical Sciences, Afe Babalola University, Ado Ekiti, Nigeria

Abstract

Investigation was carried out studying magnetic field and radiative heat transfer effects on transient MHD Prandtl-Eyring radiative, incompressible, viscous and electrically conducting non-Newtonian fluid between two fixed parallel plates filled with porous medium. The formulated physical equations were solved numerically after non-dimensionalising using finite difference scheme of Crank Nicolson and the boundary condition for the fluid at the wall was assumed to be the one of slip. Numerical findings are provided with the help of graphs to discuss the effects of various flow parameters, that is, thermal radiation parameter (N), Prandtl number (Pr), Darcy number (Da), thermal Grashof number (Gr), Magnetic field parameter wall-slip parameter (λ) as they influence the flow on velocity and temperature profiles. From the findings, it was discovered that the presence of magnetic field (M) in an electrically conducting fluid causes an increase in Lorentz force, which causes the fluid's motion to be retarded, thereby decreasing the velocity profile while increasing thermal radiation parameter (N) decreases the velocity profile and this decrease in velocity is followed by a decrease in the velocity layer. In addition, an increase in thermal Grashof number (Gr) allows the speed distribution to rise and the buoyancy force is increased by this increase while the wall-slip parameter in the lower plate gives rise to an increase in the velocity of the fluid.

Keywords

Wall-slip, Porous Plates, Prandtl-Eyring Model, Magnetohydrodynamic

Received: February 5, 2021 / Accepted: March 26, 2021 / Published online: April 16, 2021

1. Introduction

Non-Newtonian fluids are defined as fluids that have a non-linear relation between shear stress and shear strain. Shear stress is understood to be a measure of the friction force of a fluid acting on a body in that fluid's course, whereas shear stress measures angle changes in relation to two particular directions. Viscosity as a fluid property is the shear stress ratio to shear strain. Series of research work has been considered in literature in which fluid viscosity was taken to be constant. However, we find a very few examples of fluids having this property.

In certain situations, it is not always essential that the fluid viscosity is constant due to the behaviour of some fluids in nature.

There are various kinds of non-Newtonian fluid models that can be used to describe non-Newtonian fluid flow behaviours. The Power-law model, the Williamson model, the Eyring-Powell model, the Prandtl-Eyring model, the Prandtl model, and so on are examples of models, all of which have their own benefits. Owing to the difficulty of these models, researchers are running away from the study of non-Newtonian fluids.

The systematic similarity study of natural convection flows of all non-Newtonian visco inelastic fluids was investigated by Timol and Kalthia [1]. Eldabe et al. [2] researched Powell-Eyring fluid unidirectional flow between parallel plates with coupled stresses. The pulsatile flow of Powell-Eyring fluid

* Corresponding author
E-mail address: oyelamifunmilayo@abuad.edu.ng

was considered by Zueco and Beg [3]. Radiation impact of Eyring-Powell fluid on boundary layer flow over an exponentially shrinking sheet was investigated by Asmat et al. [4].

Malik et al. [5] considered the boundary layer flow of an Eyring-Powell model fluid due to a stretching cylinder with variable viscosity. Tasawar et al. [6] examined the radiation effects on the flow of Powell-Eyring fluid past a non-uniform heat source/sink unstable inclined stretching layer.

Numerical tests for the flow and heat transfer of thin film of the Powell-Eyring fluid also was considered by Khader and Megahed [7]. The steady flow in a channel with slip at the permeable limits was studied by Makinde and Osalusi [8].

The effect of radiation and heat transfer on unsteady MHD Non-Newtonian fluid flow with slip in a porous medium was studied by Gbadeyan and Dada [9]. The group theoretical similarity analysis was considered by Darji and Timol [10] to analyze natural convection boundary layer flow using non-Newtonian fluid models from Prandtl-Eyring and Williamson.

The inspiration for this research stems from the work carried out by Adesanya and Gbadeyan [11] in which the Adomian decomposition method was used to analyze the steady flow of visco-elastic fluid through a planer channel with slip.

The non-Newtonian fluid model considered in their work is the Eyring-Powell model. Oyelami and Dada [12] researched the effect of viscous dissipation on heat transfer in a porous channel through natural convection. Using the Eyring-Powell fluid model, Oyelami and Dada [13] investigated heat as well as mass transfer effects of viscous dissipation and chemical reactions. Amanullaa et al. [14] investigated MHD Prandtl fluid flow past an isothermal permeable sphere with slip effects. Numerical simulation of oscillatory oblique stagnation point flow of a magneto micropolar nanofluid was studied by Sadiq et al. [15]. Computational and physical aspects of MHD Prandtl-Eyring fluid flow analysis over a stretching sheet was analysed by Hussain et al. [16].

To the best of knowledge of the author, studies are not available in the literature studying magnetic field and radiative heat transfer effects on magnetohydrodynamic Prandtl-Eyring flow along porous plates with slip effects.

The goal of this study is to explore the transient magnetohydrodynamic Prandtl-Eyring fluid flow along porous plates with slip effects.

2. Problem Formulation

The fluid under consideration is an unsteady radiative, incompressible, viscous and electrically conducting non-Newtonian fluid between two fixed h-width parallel plates filled with porous medium. A uniform-strength magnetic field is applied perpendicular to the plate. The governing equations for the non-Newtonian fluid's unstable flow under the normal Boussinesq approximation for incompressible fluid model is given for momentum, energy and concentration equations respectively as follows:

$$\frac{\partial u^*}{\partial t^*} = -\frac{1}{\rho}\frac{\partial P^*}{\partial x^*} - \frac{1}{\rho}\frac{\partial \tau_{xy}}{\partial y^*} + g\beta_T(T^* - T_0^*) - \frac{1}{\rho}\sigma B_0^2 u^* - \frac{\nu u^*}{K} \quad (1)$$

$$\frac{\partial T^*}{\partial t^*} = \frac{k}{\rho C_p}\frac{\partial^2 T^*}{\partial y^{*2}} - \frac{1}{\rho C_p}\frac{\partial q_r}{\partial y^*} \quad (2)$$

Where u^* is the fluid velocity, t^* stands for the time, ρ represent the density, g stands for acceleration due to gravity, T^* is means fluid temperature, P^* represent fluid pressure, C_p stands for specific heat at constant pressure, β_T means coefficient of thermal expansion, k signifies the thermal conductivity, T_w^* stands for fluid temperature at $y^* = h$, T_0^* represent fluid temperature at $y^* = 0$, q_r means the radiative heat flux, σ is the electrical conductivity, υ stands for the kinematic viscosity while B_0 signifies the magnetic field and h is the distance between two plates.

The conditions of initial and boundary are given as

$$t^* = 0, u^* = 0,\ T^* = T_0^*, y \in (0, h)$$

$$t^* > 0,\ u^* = \lambda\frac{\partial u^*}{\partial y^*}, T^* = T_0^*, \text{at } y^* = 0$$

$$u^* = 0,\ T^* = T_w^*, \text{at } y^* = h \quad (3)$$

Following Cogley et al. [17] the parameter for radiation is given as

$$\frac{\partial q_r}{\partial y^*} = 4(T^* - T_0^*)L \quad (4)$$

Where L= $\int_0^\infty k\lambda_w \left(\frac{de_{b\lambda}}{dT^*}\right)_w d\lambda$, $k\lambda_w$ is the absorption coefficient and $e_{b\lambda}$ is the plank function.

By defining the non-dimensional quantities that follow,

$$X = \frac{x^*}{h}, Y = \frac{y^*}{h}, U = \frac{u^*}{u_0^*}, t = \frac{t^* u_0^*}{h}, P = \frac{P^*}{\rho u_0^{*2}}, T = \frac{T^* - T_0^*}{T_w^* - T_0^*}, Re = \frac{hu_0^*}{\nu}, Ec = \frac{u_0^{*2}}{Cp(T_w^* - T_0^*)},$$

$$N = \frac{4Lh^2}{k}, Pr = \frac{\rho Cp\nu}{k}, Da = \frac{h^2}{K}, Gr = \frac{g\beta_T(T_w^* - T_0^*)h^2}{\nu}, M^2 = \frac{\sigma B_0^2 h^2}{\rho\nu} \quad (5)$$

Introducing equation (4) under the expression in equations (5) into equations (2) gives

$$Re\frac{\partial T}{\partial t} = \frac{1}{Pr}\frac{\partial^2 T}{\partial Y^2} - \frac{N}{Pr}T \quad (6)$$

under the corresponding dimensionless boundary conditions

$$t = 0, U = 0, T = 0, y \in (0, h)$$

$$t > 0, U = \lambda \frac{\partial U}{\partial Y}, T = 0, \text{at } Y = 0$$

$$U = 0, T = 1, \text{at } Y = 1 \quad (7)$$

The Prandtl-Eyring visco-elastic model is given by Darji and Timol [10] as

$$\tau_{xy} = \beta sinh^{-1}\left(\frac{1}{b}\frac{\partial u^*}{\partial y^*}\right) \quad (8)$$

where τ_{xy} represents the shear stress, $\frac{\partial u^*}{\partial y^*}$ stands for velocity gradient, $\beta$and b signifies Prandtl-Eyring parameters.

Taking the hyperbolic sine function approximation in the first and second order gives

$$\sin h^{-1}\left(\frac{1}{b}\frac{\partial u^*}{\partial y^*}\right) \cong \frac{1}{b}\frac{\partial u^*}{\partial y^*} - \frac{1}{6}\left(\frac{1}{b}\frac{\partial u^*}{\partial y^*}\right)^3, \left|\frac{1}{b}\frac{\partial u^*}{\partial y^*}\right| \ll 1 \quad (9)$$

The Prandtl-Eyring model stress tensor is given as

$$\tau_{xy} = \frac{\beta}{b}\frac{\partial u^*}{\partial y^*} - \frac{\beta}{6}\left(\frac{1}{b}\frac{\partial u^*}{\partial y^*}\right)^3 \quad (10)$$

The momentum equation for the Prandtl-Eyring model becomes the momentum equation when equations (5) and (10) are introduced into equation (1). This is given as

$$Re\frac{\partial U}{\partial t} = -\frac{\partial P}{\partial X} + \left[\xi - \eta\left(\frac{\partial U}{\partial Y}\right)^2\right]\frac{\partial^2 U}{\partial Y^2} + G_r T - (M^2 + Da)U \quad (11)$$

Where $\xi = \frac{\beta}{b\mu}$ and $\eta = \frac{\beta U_0^{*4}}{2\rho v^3 b^3}$ are the characteristics of Prandtl-Eyring model.

where $\frac{\partial P}{\partial X} = \text{constant}$, U represents dimensionless velocity, t stands for dimensionless time, T signifies dimensionless temperature function, N becomes the thermal radiation heat transfer parameter, Pr becomes the Prandtl number, Da represents Darcy number, Re signifies the Reynold number, Gr the thermal Grashof number, M signifies the Magnetic field parameter and λ stands for wall-slip parameter.

3. Numerical Solution

The equations of finite difference corresponding to the equations (11) and (6), respectively, are

$$Re\frac{U_j^{k+1} - U_j^k}{\Delta t} = \left[\xi - \eta\left(\frac{U_{j+1}^k - U_{j-1}^k}{2\Delta Y}\right)^2\right]\left[\frac{U_{j-1}^{k+1} - 2U_j^{k+1} + U_{j+1}^{k+1} + U_{j-1}^k - 2U_j^k + U_{j+1}^k}{2(\Delta Y)^2}\right] + G_r\left(\frac{T_j^{k+1} + T_j^K}{2}\right) - (M^2 + Da)\left(\frac{U_j^{k+1} + U_j^k}{2}\right) \quad (12)$$

$$Re\frac{T_j^{k+1} - T_j^k}{\Delta t} = \frac{1}{pr}\left[\frac{T_{j-1}^{k+1} - 2T_j^{k+1} + T_{j+1}^{k+1} + T_{j-1}^k - 2T_j^k + T_{j+1}^k}{2(\Delta Y)^2}\right] - \frac{N}{Pr}\left[\frac{T_j^{k+1} + T_j^k}{2}\right] \quad (13)$$

With the following boundary conditions

$$U_j^{k+1} = 0, u_j^k = 0, T_j^{k+1} = 0, T_j^k = 0, \forall\, j, t = 0$$

$$U_{j-1}^{k+1} = \frac{-2\Delta Y U_j^{k+1}}{\lambda} + U_{j+1}^{k+1}, T_{j-1}^{k+1} = 0, j = 1, t > 0$$

$$U_{j-1}^k = \frac{-2\Delta Y U_j^k}{\lambda} + U_{j+1}^k, T_{j-1}^k = 0, j = 1, t > 0$$

$$U_j^{k+1} = 0, T_j^{k+1} = 1, U_j^k = 0, T_j^k = 1, j = n, t > 0 \quad (14)$$

where U_0 and T_0 are the velocity and temperature at $Y = 0$ respectively, U_n and T_n are the velocity and temperature at $Y = 1$ respectively and the interval $\Delta Y = \frac{1}{n}$.

Subscript j and superscript k specify grid points along the paths Y and t respectively in the calculations. At all grid points at t=0 from the initial conditions, the values of U and T are defined. At the (k+1)th time level, the calculation of U and T using the known values at the previous (k)th time level is evaluated as follows:

By forming a tri-diagonal system of equations from the equations of finite difference (12) and (13), the values of T at each nodal point at the next step length were calculated using previously established values. Due to the large performance involved, the Thomas algorithm was used to overcome this tri-diagonal equation system with the aid of the MATLAB programming kit.

As such, the values of T are determined on a certain j at the (k+1)th time level at each nodal point. Usage of the T values in Eq at the (k+1)th time step. (13), the values of U are similarly determined at the (k+1)th time step. The values of T and U are thus known at a basic j-level.

4. Results and Discussion

Numerical findings are provided with the help of graphs to discuss the effect of different physical parameters on the temperature and velocity profiles. Except when it varies on a specific graph, every graph corresponds to these values. $\xi = 1, \eta = 1$, Gr=1, M=1, $\lambda = 1$, Da=1, Re=1, Pr=1, N=1.

The velocity profile for various values of Prandtl-Eyring parameter ξ is shown in Figure 1. It is found that the velocity profile is reduced by increasing parameter ξ while on figure 2, the effect of Prandtl-Eyring Parameter η on the velocity causes the velocity profile to increase.

Figure 3 shows that the presence of M in an electrically conducting fluid results in an increase in the Lorentz force, which causes the fluid's motion to be retarded, thus reducing the velocity profile.

For different values of thermal Grashof number Gr, Figure 4 shows the velocity distribution. An rise in Gr allows the distribution of speed to increase and this increase increases the buo buoyancy force.

In showing the effects of thermal radiation parameters on the velocity and temperature profiles, figures 5 and 6 show that increasing thermal radiation parameters decreases the velocity profile and this decrease in velocity is followed by a decrease in the velocity layer while on the temperature profile, it is noted that there is a drop in fluid temperature as the thermal radiation parameter rises, which is physically true since radiation removes heat from the body.

Figure 7 shows the velocity profile defined by the Darcy number Da for the different porosity parameter values. By reducing the permeability of the porous medium, increasing the amount of Darcy reduces the velocity profile.

Figure 8 shows that an increase in the wall-slip parameter in the lower plate gives rise to an increase in the velocity of the fluid.

The effect of the velocity and temperature profiles of Prandtl number Pr is stated in figures 9 and 10, respectively. A rise in the amount of Prandtl allows the thermal state to decrease, since the lower value of Pr increases the thermal conductivity of the fluid temperature. This decrease was experienced. Both velocity and temperature profiles are decreased by this rise in Pr.

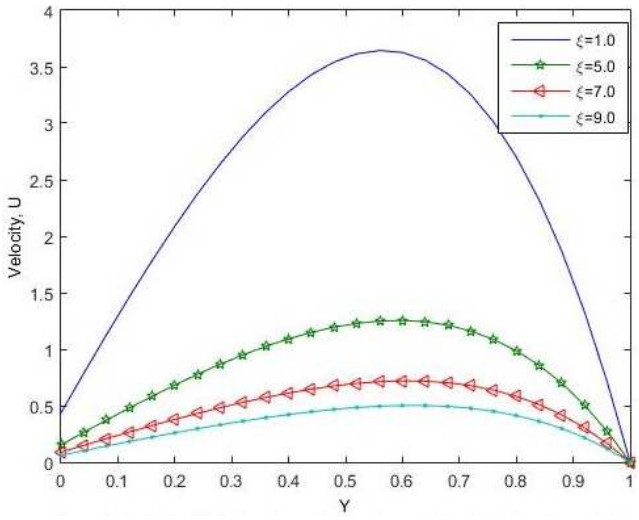

Figure 1. Velocity distribution for various values of Prandtl-Eyring Parameter ξ.

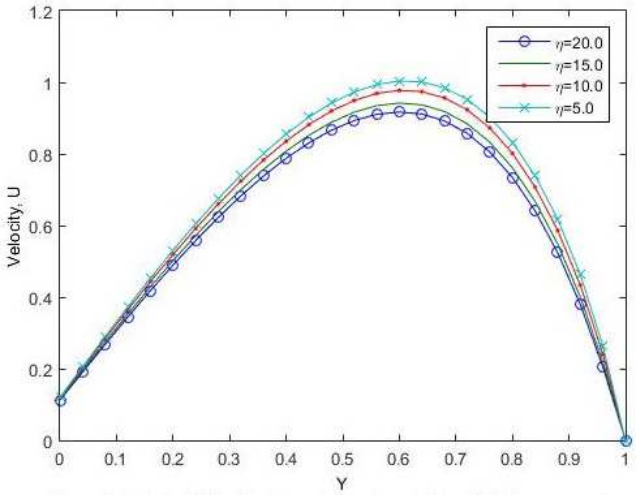

Figure 2. Velocity distribution for various values of Prandtl-Eyring Parameter η.

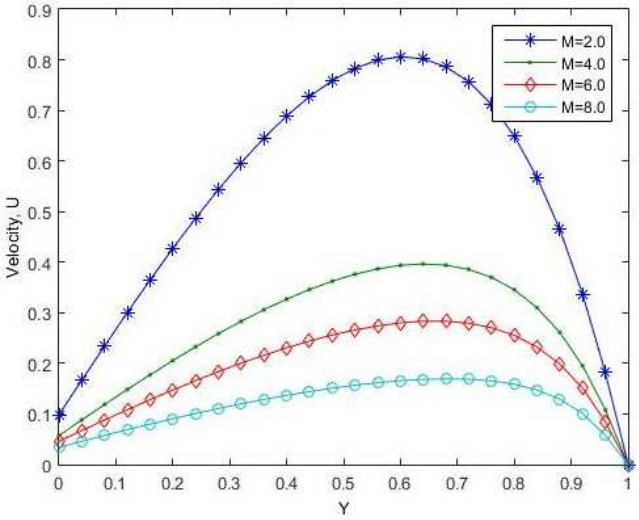

Figure 3. Velocity distribution for various values of Magnetic field Parameter M.

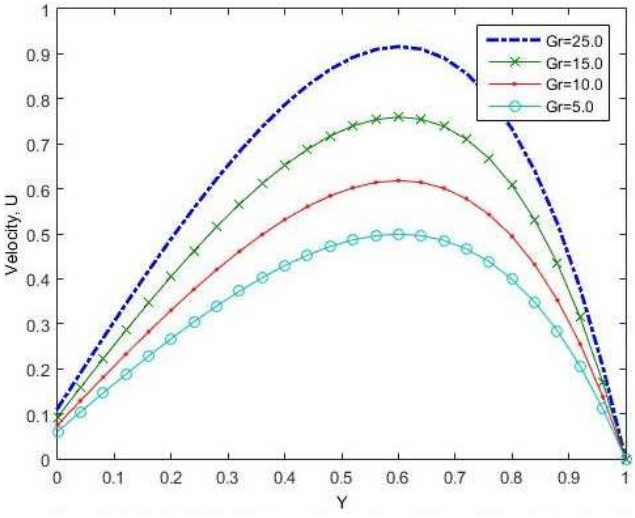

Figure 4. Velocity distribution for various values of thermal Grashof number Gr.

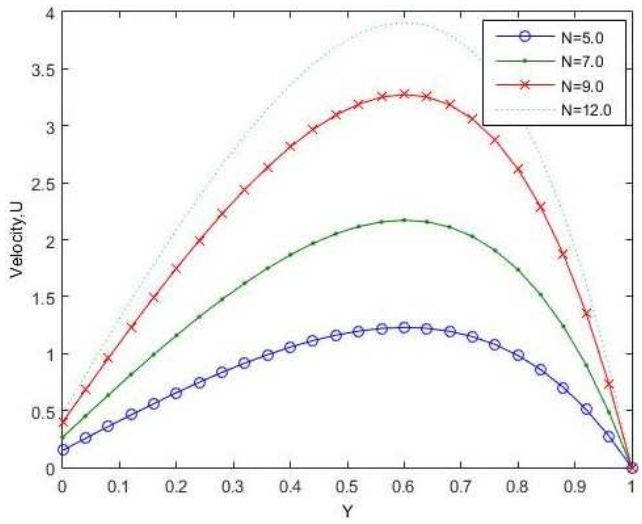

Figure 5. Velocity distribution for various values of thermal radiation N.

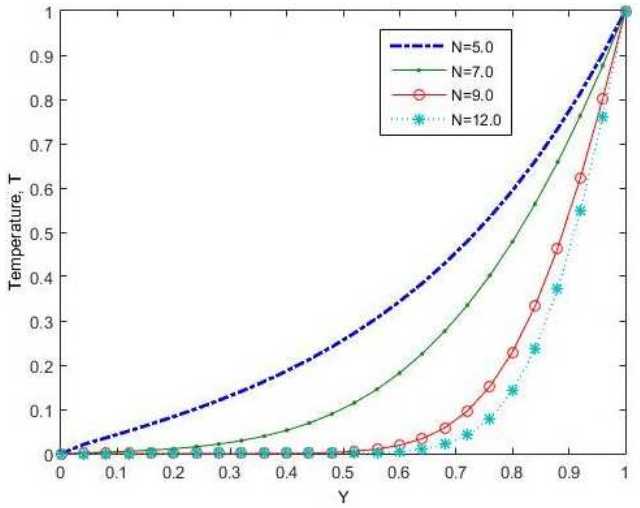

Figure 6. Temperature distribution for various values of thermal radiation N.

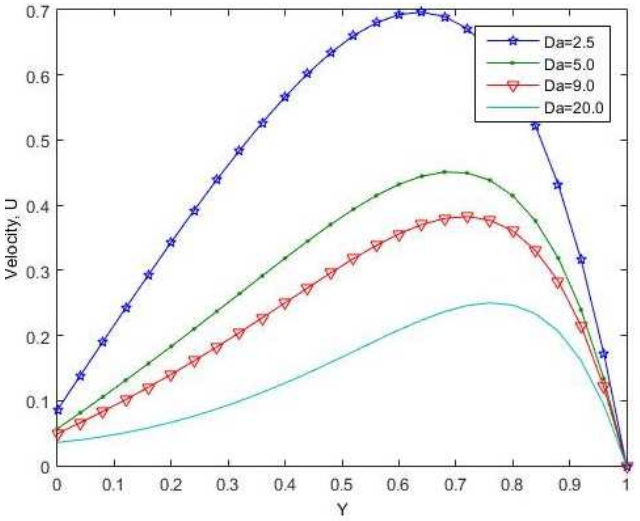

Figure 7. Velocity distribution for various values of Darcy number Da.

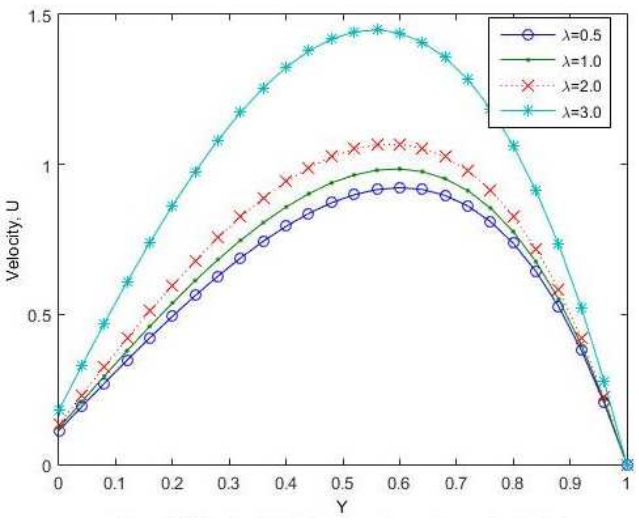

Figure 8. Velocity distribution for various values of wall slip λ.

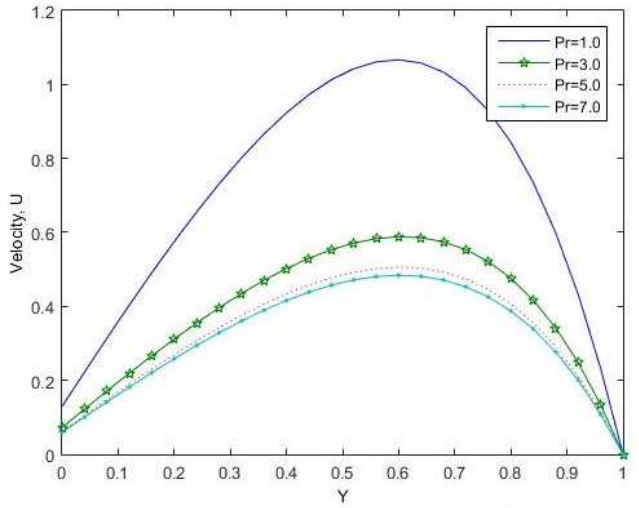

Figure 9. Velocity distribution for various values of Prandtl number Pr.

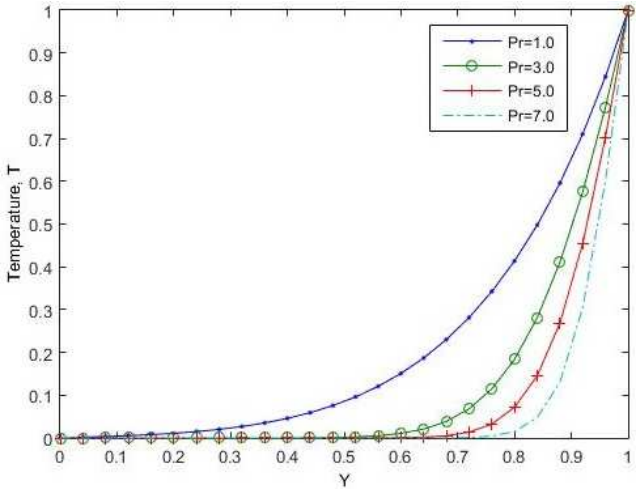

Figure 10. Temperature distribution for various values of Prandtl number Pr.

5. Conclusion

An unsteady radiative, incompressible, viscous and electrically conducting non-Newtonian fluid between two fixed h-width parallel plates filled with porous medium. Numerical findings are provided with the help of graphs to discuss the effect of different physical parameters on the temperature and velocity profiles. The findings are

The velocity profile is decreased by rising thermal radiation parameters and this decrease in velocity is followed by a decrease in the velocity layer as there is a decrease in fluid temperature as the thermal radiation parameter increases on the temperature profile.

The presence of M in an electrically conducting fluid results in an increase in the Lorentz force, which causes the fluid's motion to be retarded, thereby decreasing the velocity profile.

Increasing thermal radiation parameters decreases the velocity profile and this decrease in velocity is followed by a decrease in the velocity layer.

An increase in Gr allows the speed distribution to rise and the buoyancy force is increased by this increase.

The wall-slip parameter in the lower plate gives rise to an increase in the velocity of the fluid.

A rise in the amount of Prandtl allows the thermal state to decrease

References

[1] M. G. Timol, N. L. Kalthia. (1985). Group theoretic approach to similarity solutions in non-Newtonian natural convection flows, *Journal of Energy Heat and Mass Transfer*, 7 (4), 251-288.

[2] N. T. M. Eldaebe, A. A. Hassan, A. A. Mona. (2003). Effect of couple stresses on the MHD of a non-Newtonian unsteady flow between two parallel porous plates, *Journal of physics*, 58a, 204-210.

[3] J. Zueco, O. A. Beg. (2009), Network numerical simulation applied to pulsatile non-Newtonian flow through a channel with couple stress and wall mass effects, *International Journal of Applied Mathematics and Mech*., 5 (2), 1-16.

[4] Asmat, A. K. Najeeb, K. Hassan, S. Faqiha. (2014). Radiation effects on boundary layer flow of an Eyring-Powell fluid over an exponentially shrinking sheet, *Ain Shams Engineering Journal*, 5, 1337-1342.

[5] M. Y. Malik, A. Hussian, Nadeems. (2013). Boundary layer flow of an Eyring-Powell model fluid due to a stretching cylinder with variable viscosity, *Journal of Scientia iranica,* 20 (2), 313-321.

[6] H. Tasawar, A. Sadia, M. Maraj, A. Ahmed. (2014). Radiation effects on the flow of Powell-Eyring fluid past an unsteady inclined stretching sheet with non- niform Heat Source/Sink, *PLOS ONE 9 (7): e103214. doi: 10.1371/journal.pone.0103214*.

[7] M. M. Khader, A. M. Megahed. (2013). Numerical studies for flow and heat transfer of the Powell-Eyring fluid thin film over an unsteady stretching sheet with internal heat generation using the chebyshev finite difference method, *Journal of Applied Mechanics Technical Phys*, 5 (4), 44-50.

[8] O. D Makinde, E Osalusi. (2006). MHD steady flow in a channel with slip at the permeable boundaries, *Romania Journal of Physics,* 51 (3-4), 319-328.

[9] J. A. Gbadeyan, M. S. Dada. (2013). On the Influence of radiation and heat transfer on an unsteady MHD Non-Newtonian fluid flow with slip in a porous medium, *Journal of Mathematical Research*, 5 (3), 40-49.

[10] R. M. Darji, M. G. Timol. (2013). Group-Theoretic Similarity Analysis for Natural Convection Boundary Layer Flow of a Class of Non-Newtonian Fluids, *International Journal of Advanced Scientific and Technical Research,* 3 (1), 54-69.

[11] S. O. Adesanya, J. A. Gbadeyan. (2011). Adomia Decomposition approach to steady visco-elastic flow with slip through a planar channel, *Journal of nonlinear science,* 11 (1), 86-94.

[12] F. H. Oyelami, M. S. Dada (2018). Unsteady magnetohydrodynamic flow of some non-Newtonian fluids with slip in a porous channel, International Journal of Heat and Technology, vol. 36, (2), 709-713. https://doi.org/10.18280/ijht.360237

[13] F. H. Oyelami, M. S. Dada (2018). Numerical analysis of non-Newtonian fluid in a non-Darcy porous Channel, Modelling, measurement and control, 87 (2), 83-91. https://doi.org/10.18280/mmc_b.870204

[14] C. H. Amanullaa, S. Saleemb, Abderrahim Wakifc, M. M. AlQarnib. (2019). MHD Prandtl fluid flow past an isothermal permeable sphere with slip effects, Case Studies in Thermal Engineering, 14, 100447.

[15] M. A. Sadiq, A. U. Khan, S. Saleem, S. Nadeem. (2019). Numerical simulation of oscillatory oblique stagnation point flow of a magneto micropolar nanofluid, RSC Adv. 9, 4751–4764.

[16] A. Hussain, M. Y. Malik, M. Awais, T. Salahuddin, S. Bilal. (2019). Computational and physical aspects of MHD Prandtl-Eyring fluid flow analysis over a stretching sheet, Neural Comput & Applic, 31 (Suppl 1): S425–S433. DOI 10.1007/s00521-017-3017-5.

[17] A. C. Cogley, W. C. Vincenti, S. E. Gilles. (1968) Differential Approximation for Radiative Transfer in a Non-Grey Gas near Equilibrium, *AIAA Journal*, 6 (3), 551-553.